

Liquid waveguide capillary cell for the spectrophotometric determination of nanomolar iodate concentrations in marine waters

Jianrong Lin^{1*}

¹ Key Laboratory of Estuarine Ecological Security and Environmental Health of Fujian Province University, Tan Kah Kee College, Xiamen University, Zhangzhou 363105, China

Received 31 January 2021; accepted 20 May 2021

© Chinese Society for Oceanography and Springer-Verlag GmbH Germany, part of Springer Nature 2022

Abstract

A new spectrophotometric method based on a liquid waveguide capillary cell for an enhanced detection was developed to measure nanomolar iodate concentrations. This method has a detection limit and precision of 1–2 nmol/L, which is equivalent to 10% that of conventional methods, a recovery of 97.7%–104.0%, and a working range of 10–120 nmol/L. Water samples were collected from three estuaries and one coastal ocean for testing, and the proposed technique detected as low as 11 nmol/L and 18 nmol/L iodate in these samples. This newly developed method is helpful in understanding the biogeochemical cycle of iodine in nature.

Key words: iodate, liquid waveguide capillary cell, spectrophotometric determination

Citation: Lin Jianrong. 2022. Liquid waveguide capillary cell for the spectrophotometric determination of nanomolar iodate concentrations in marine waters. *Acta Oceanologica Sinica*, 41(3): 103–108, doi: 10.1007/s13131-021-1921-0

1 Introduction

Inorganic dissolved iodine exists as iodide and iodate in seawater (Wong, 1991). Iodate is the major species and can be found rather ubiquitously in the oceans (Cutter et al., 2018; Moriyasu et al., 2020; Tian et al., 1996; Truesdale, 1994; Truesdale and Bailey, 2002; Tsunogai, 1971; Tsunogai and Henmi, 1971; Wong, 1976, 1991, 1995; Wong and Cheng, 2008; Wong and Zhang, 2003). The concentrations of iodate in open ocean waters range mostly between 200 nmol/L and 500 nmol/L. Low concentrations are found in the surface mixed layer where iodate is slightly depleted (Wong, 1991; Wong and Brewer, 1974; Wong et al., 1976).

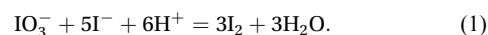
Two conventional methods have been used extensively for the direct determination of iodate in these waters. In one technique, iodate is reacted with excess iodide under acidic conditions to form tri-iodide ion, which may then be quantified either through titrimetry or spectrophotometry (Chapman and Liss, 1977; Dubravčić, 1955; Moriyasu et al., 2020). As an alternative, iodate may be determined directly through differential pulse polarography (Herring and Liss, 1974).

The precision of both methods is approximately $\pm 5\%$ or ± 10 nmol/L. Other techniques have also developed based on inductively coupled plasma mass spectrometry coupled with gel electrophoresis, headspace gas chromatography or reverse phase liquid chromatography (Brüchert et al., 2007; Moriyasu et al., 2020; Xie et al., 2019; Zhang et al., 2018); however, these approaches are burdened by the associated high maintenance cost of this detection system.

The precisions and detection limits of conventional methods are quite adequate for determining iodate distribution in open oceans. However, iodate concentration decreases in areas near the coasts and can easily drop below 50 nmol/L, which is even lower than the detection limits for inshore and estuarine waters

(Guo and Peng, 1989; Smith and Butler, 1979; Ullman et al., 1988). For these cases, the existing methods become marginal to inadequate. The dissolved iodine may also exist as dissolved organic iodine (DOI), which is especially plentiful in coastal waters where the concentration of iodate is usually low (Schwehr and Santschi, 2003; Wong and Cheng, 1998, 2001, 2008). To date, no analytical method has been developed to directly measure DOI, which is instead estimated as the difference in concentration between total dissolved iodine and the sum of iodide and iodate. Thus, the precision and detection limit in iodate determination will be carried directly into the estimation of DOI concentration. Given that DOI concentrations are mostly at or below 0.1 $\mu\text{mol/L}$, a method for iodate determination with a precision of lower than $\pm 0.01 \mu\text{mol/L}$ and a detection limit below 0.01 $\mu\text{mol/L}$ is urgently needed.

The principle of iodate determination through spectrophotometry is as follows:



In acidic solution, iodate first reacts with iodide and, the produced I_2 can be further reacted with iodide to form tri-iodide. At 298 K, the reaction constant of reaction Eq. (2) is 725 L/mol, e.g., when iodide concentration is 16 mmol/L, I_2 accounts for only 4%, and tri-iodide accounts for over 96% (Pai et al., 1993). When iodide is dissolved in water, the absorption peaks of the molecular iodine and tri-iodide are at 450 nm and 353 nm, respectively (Pai et al., 1993).

According to Lambert–Beer's law, the total absorbance con-

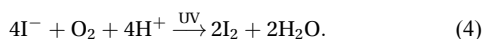
sists of molecular iodine and tri-iodide as follows:

$$A = \varepsilon_{I_2} b c_{I_2} + \varepsilon_{I_3^-} b c_{I_3^-}, \quad (3)$$

where A is the absorbance, ε_{I_2} and $\varepsilon_{I_3^-}$ represent the molar absorptivity of I_2 and I_3^- , respectively, unit is $L/(\text{mol}\cdot\text{cm})$; b is the path-length (cm); and c_{I_2} and $c_{I_3^-}$ are the concentrations of I_2 and I_3^- (mol/L), respectively. When 353 nm is chosen, the absorbance of molecular iodine can be neglected in an excess of iodide solution.

In conventional spectrophotometry, the upper limit of the path length of the spectrophotometer cell is usually 10 cm. The liquid waveguide capillary cell (LWCC) with path lengths of up to 100 cm is now available. In theory, the detection limit of a spectrophotometric method may then be reduced by an order of magnitude.

Air oxidation of iodide is a long-recognized interference in iodometry (Carpenter, 1965), and the reaction rate is accelerated by light (especially ultraviolet light, UV) in the reaction (Fitzmaurice and Frei, 1991). The reaction equation is as follows:



Equation (4) is an important problem in the determination of iodate nanomolar quantities. The absorbance of tri-iodide formed from iodate per unit concentration of iodate per unit path length is estimated to be only $\sim 7.0 \times 10^4 L/(\text{mol}\cdot\text{cm})$ from the reported molar absorptivity of tri-iodide in seawater. Air oxidation may occur in the test solution under favorable acidic condition, even rapidly when the test solution is exposed to the light source in the spectrophotometer. Given that the absorbance is measured at 353 nm, the test solution is exposed to near-UV light. In conventional spectrophotometry, the test solution is exposed to a monochromatic light source at that wavelength, and the exposure time when absorbance is read is short, usually in seconds. Thus, the effect is minimal (e.g., the absorbance is stable for at least 1 h, data not shown). When a LWCC is used, the incident light from the deuterium lamp is not fractionated through a monochromator before passing through the test solution. As a result, the test solution is exposed to the full UV spectrum, including the energetic short wavelength UV light of the deuterium lamp, and the exposure time is prolonged until the absorbance is read for 1 min and averaged to minimize the effect of noise. In addition, air oxidation may also occur in the KI solution even before being added to the test solution. This effect can be counteracted by measuring the reagent blank. KI air oxidation increases the absorbance of the sample solution; hence, the iodate in the sample will be overestimated. To reduce KI oxidation, the method must optimize the KI stock solution to maintain the conditions of the sample, reaction solution, and measurement.

Two interferences must also be considered. One is chromophoric dissolved organic matter (CDOM), also known as “gelbstoff” or yellow substances (Bricaud et al., 1981), which is responsible for UV and low wavelength visible light attenuation in a wide range of natural waters (Guo et al., 2007). If CDOM is not subtracted, then the solution absorbance will increase, and the iodate concentration will be overestimated. As a solution, the blank of a sample (B_s) is measured and subtracted. Given that the sample for a chemical reaction is acidified, the sample for B_s measurement must also be acidified. Whether B_s changes with time must be examined. In addition, H_2O_2 participates in the reaction to oxidize KI, and the degree of overestimation decreases with the reduction of H_2O_2 concentration in the sample. Redu-

cing the H_2O_2 concentration of the sample is another challenge that must be addressed.

Operational problems that are insignificant in conventional spectrophotometry may become significant when a LWCC system is used. Here, the problems associated with the conventional spectrophotometric method for iodate detection in marine waters were examined and circumvented to ensure that the proposed technique can be adapted to a LWCC system for iodate determination at the nanomolar level.

2 Experiments

2.1 Reagents and solutions

All solutions are prepared using analytical reagent-grade chemicals and reagent-grade water. In brief, 2 mmol/L KIO_3 stock solution is prepared by dissolving 0.0428 g of potassium iodate, which has been dried at a 110°C oven for 2 h in reagent grade water and then diluted to 100 mL. Standard 0.5 $\mu\text{mol/L}$ KIO_3 solution is prepared by diluting the KIO_3 stock solution.

The mixed acid solution contains 0.1 mol/L sulfuric acid and 1% (*w/w*) sulfamic acid. Na_2CO_3 stock solution of 0.1 mol/L is prepared by dissolving 1.06 g of Na_2CO_3 and diluting to a final volume of 100 mL. Na_2CO_3 solution of 10^{-3} mol/L is prepared by pipetting 10 mL of 0.1 mol/L Na_2CO_3 stock solution then diluting to a final volume of 1 L. Daily fresh reagent 10% (*w/w*) KI solution is prepared by dissolving 2 g of KI, which has been dried in an 80°C oven for 2 h in 18 g of 10^{-3} mol/L Na_2CO_3 solution. The intermediate of artificial seawater is prepared following the method of Lyman and Fleming (1940).

2.2 Apparatus

The TIDAS system includes a 100 cm liquid waveguide capillary cell (LWCC, WPI Inc., USA), a deuterium halogen light source (DH-2000-BAL, Micropack, Germany), an Ocean Optics TIDAS spectrophotometer, and a high precision multichannel pump (ISMATEC, Switzerland) for sample introduction.

The pH meter model is Thermo Scientific Model Orion 3-star pH meter mounted with an 8102B electrode.

The detector is controlled through a personal computer running SPECTRAL 2.0 (Ocean Optics, USA) software.

2.3 Procedure

A calibration curve is constructed by iodate standard solution in the range of 0.01–0.1 $\mu\text{mol/L}$ and then diluted to 50 mL in separate 50 mL volumetric flasks. These mixtures are treated as the samples. For natural samples, an aliquot of 50 mL of the sample is also transferred into a 50 mL volumetric flask, followed by the addition of 1 mL of mixed acid solution. The mixture is allowed to stand for 10 min with intermittent swirling to ensure that any nitrite present may be destroyed by the added sulfamic acid. An aliquot of 2 mL of 10% (*w/w*) KI is then added, and the mixture is allowed to stand for another 5 min before being pumped into the TIDAS system for absorbance measurement.

Before the sample's absorbance is measured, the sample is pumped and flowed through the system for 0.5 min to flush any residue and then measured at 353 nm for another 1 min at a sampling frequency of 1 datum/s. Each sample needs an additional 1.5 min to finish measuring its absorbance, thus prolonging the next sample's waiting time. In addition, the side reaction will increase their absorbance. As a solution, a time delay of 1.5 min for the next sample is set to eliminate the side reaction effect.

The concentration of iodate in the sample is then calculated from the following Eq. (5):

$$C_s = (A - B_s - B_r)/S, \quad (5)$$

where C_s is iodate concentration in the sample, A is the absorbance of the sample, B_s is the sample blank due to the CDOM, B_r is the reagent blank, and S is the slope of the working curve.

3 Results and discussion

3.1 Optimizations to reduce KI air oxidation

Physical parameters such as pump speed, reaction time, and chemical parameters such as reagent concentrations were investigated to optimize the system. The univariate method was used, i.e., only one parameter varied while the other reaction conditions are similar.

Sodium carbonate does not disturb the reaction or the measurement of tri-iodide and hence can be used to adjust the pH of the KI stock solution to prevent KI air oxidation. Figure 1 shows that the pH of KI (10%, *w/w*) stock solution was 10.68, 9.33, and 7.06, stocked in 10^{-3} , 10^{-4} , and 0 mol/L sodium carbonate solution, respectively. When the pH was 10.68, the absorbance was 0.068 ± 0.003 ($n=8$) for eight measurements within 12 h. Given the small standard deviation, the absorbance almost did not change within 12 h. This condition is ideal because the samples are typically measured within 30 min of KI addition. On the contrary, the absorbance increasing rate was 0.008 h^{-1} (1.2 nmol/L iodate per hour) in pH 9.33 solution and exhibited an accelerated trend in pH 7.06. In general, the rate followed the equation of $A = 4 \times 10^{-4} t^3 - 3.9 \times 10^{-3} t^2 + 2 \times 10^{-2} t + 5.27 \times 10^{-2}$, $R^2 = 0.994$ (A is absorbance; t is the preserving time, h).

In Eqs (1) and (2), $0.2 \mu\text{mol/L}$ iodate was added to ensure that KI concentration was sufficient for real sample measurement. This amount is larger than the method's upper limit ($0.1 \mu\text{mol/L}$). Hence, any KI concentration that has been tested here is sufficient for the natural sample measurement.

The KI concentration optimization test (Fig. 2) shows that when KI concentration was larger than 24 mmol/L , the absorbance reached its climax and remained constant. At this point, the effect of increasing the KI concentration will be null. Hence, KI concentration of 24 mmol/L was chosen.

Acidity test shows that when pH was less than 3.5, the acidity was sufficient to start the main reaction (Fig. 2b). The KI contact time test shows that the main reaction was completed after 2.5 min and did not change for at least the next 30 min. A 5 min reaction time was chosen to ensure the consistency of the reaction.

Pump speed is relevant to the residence time of the sample.

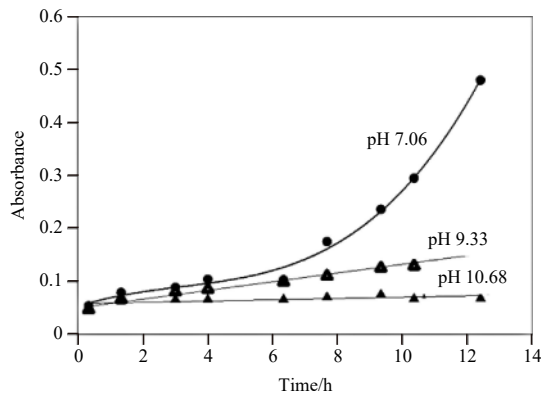


Fig. 1. Relationship between the stock time and the extent of the air oxidation (absorbance) of the stock solution kept in various of pH [10% (*w/w*)].

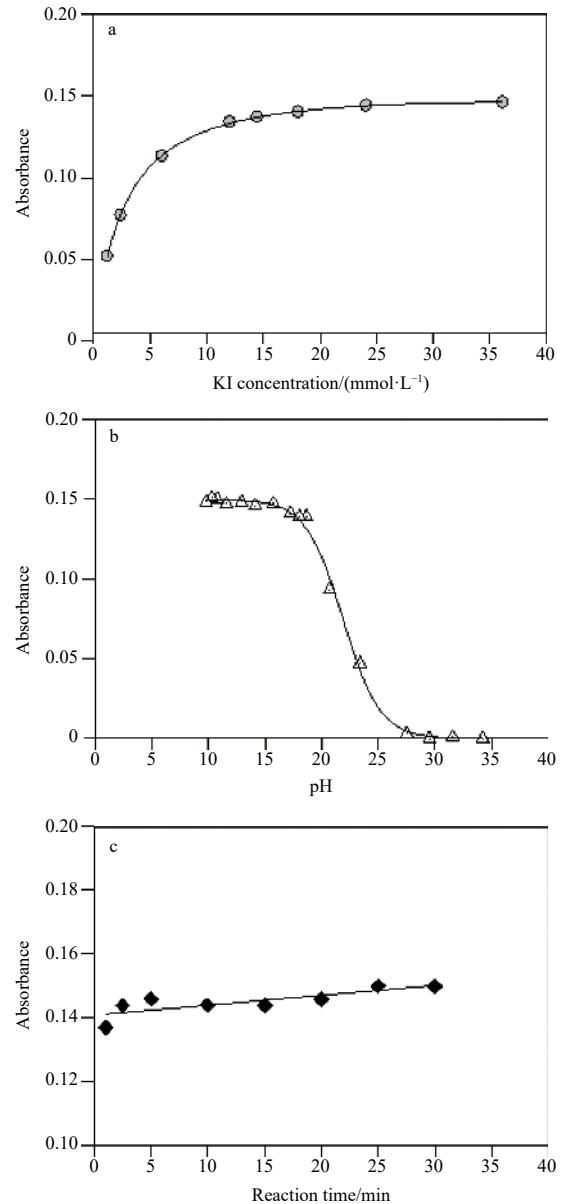


Fig. 2. Relationship between extent of KI air oxidation (absorbance) and KI concentration ($[\text{IO}_3^-]=0.2 \mu\text{mol/L}$, 10 cm cell, pH=3, KI contact time is 5 min) (a), pH ($[\text{IO}_3^-]=0.2 \mu\text{mol/L}$, 10 cm cell, $[\text{KI}]=24 \text{ mmol/L}$, KI contact time is 5 min) (b), and KI contact time ($[\text{IO}_3^-]=0.2 \mu\text{mol/L}$, 10 cm cell, pH=3, $[\text{KI}]=24 \text{ mmol/L}$) (c) in iodate reduced reaction.

On the one hand, a low residence time can reduce UV exposure time. On the other hand, a low residence time is correlated to a high pump speed and a high flow rate. Under these conditions, exquisite turbulence will be generated inside, and the absorbance will be unstable.

Figure 3 shows the relationship among pump speed, residence time, and absorbance of $0.05 \mu\text{mol/L}$ KIO_3 reaction solution. When the pump speed ranged from 10 r/min to 30 r/min, the sample residence time was reduced drastically from $\sim 9 \text{ s}$ to $\sim 5 \text{ s}$. In addition, the absorbance of a $0.05 \mu\text{mol/L}$ KIO_3 solution ($0.15 \mu\text{mol/L}$ I_3^-) decreased by ~ 0.2 . From 30 r/min to 100 r/min, the residence time decreased slowly from $\sim 5 \text{ s}$ to $\sim 4 \text{ s}$. The reduction in residence time became insignificant when the pump speed was larger than 60 r/min. The variation of absorbance due

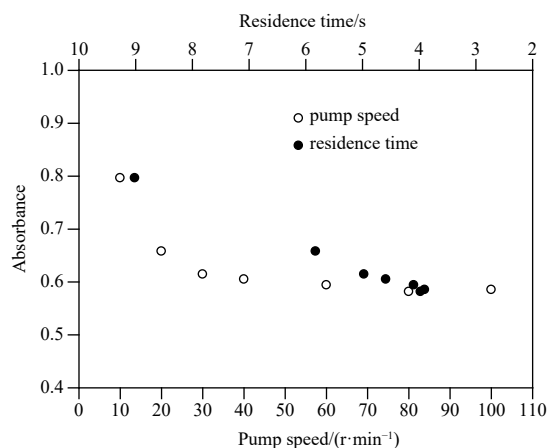


Fig. 3. Relationship among pump speed, residence time, and absorbance in LWCC; $[\text{IO}_3^-]$ is 0.05 $\mu\text{mol/L}$.

to the increase in pump speed can be neglected, and the turbulence was increased due to the high flow rate. Therefore, the optimized pump speed (30–40 r/min) was selected.

3.2 Interferences of sample blank and H_2O_2

The relationship between time and sample absorbance was analyzed (Fig. 4). The blank values of a sample (B_s) were reduced by subtracting the absorbance of each sample after the sample was acidified. The B_s of the solution slightly decreased after acidification, and the blank remained stable at least for 1 h.

The relationship of the oxidation ability of H_2O_2 with KI, pH, and reaction time was also examined (Fig. 5). The results show a positive relationship between absorbance and KI concentration or reaction time but a negative relationship between absorbance and pH. When the KI concentration increased from 1 mmol/L to 36 mmol/L, the absorbance increased by 0.1 only. When pH increased from 2.5 to 6.0, the absorbance decreased only by ~0.01. By contrast, when reaction time increased from 1 min to 30 min, the absorbance increased sharply. Hence, the reaction time is the main controlling factor for the increasing absorbance. Decreasing the contact time is the most effective way to diminish H_2O_2 interference.

Without the catalyst, approximately 2%–4% of H_2O_2 can participate in the reaction and produce I_2 :

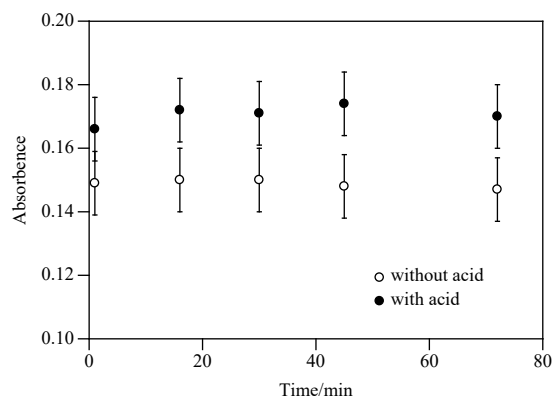
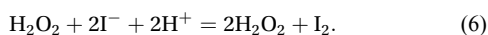


Fig. 4. Relationship between absorbance and time with/without acid of a sample blank.

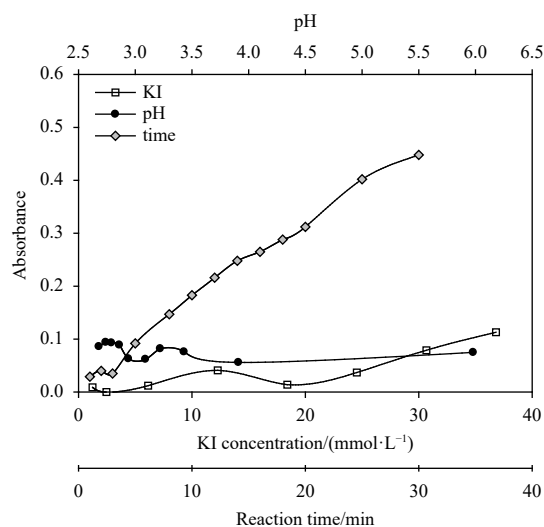


Fig. 5. Relationship between the absorbance and KI concentration (a), pH (b) and reaction time (c); the H_2O_2 concentration in the solution is 0.5 $\mu\text{mol/L}$.

The hydrogen peroxide concentration in shelf sea and estuary varies from 0.05 $\mu\text{mol/L}$ to 5 $\mu\text{mol/L}$ (Kieber and Helz, 1992; Wu et al., 2015) and increases when approaching near the shore. Concomitantly, iodate concentration decreases, and the interference increases toward the shore. According to Eq. (6), hydrogen peroxide interference should not be neglected in the low iodate zone.

A time series experiment was conducted to test the decreasing rate of H_2O_2 in the sample. The results show that $[\text{H}_2\text{O}_2]$ decreased from 0.14 $\mu\text{mol/L}$ to 0.02 $\mu\text{mol/L}$ within 4 d (Fig. 6). A simple calculation shows that 0.02 $\mu\text{mol/L}$ $[\text{H}_2\text{O}_2]$ can produce absorbance that is equal to 1–2 nmol/L iodate. Therefore, if the sample is stored for 4 d, then the hydrogen peroxide influence becomes negligible.

3.3 Analytical performance

The analytical performance of this method was investigated under optimal conditions. The calibration curve of iodate standard was examined within the concentration range of 0.01–0.12 $\mu\text{mol/L}$ in the mediate of artificial seawater. The corresponding calibration curve is shown in Fig. 7, $y=(6.89\pm 0.08)x+(0.272\pm 0.005)$, $R^2=0.9997$, $\varepsilon=(22\ 958\pm 285)$ L/(mol·cm). The molar ab-

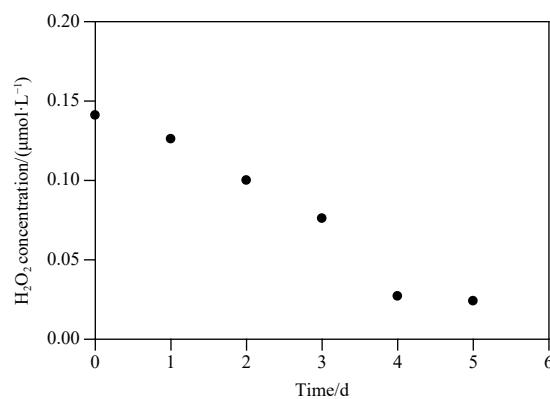


Fig. 6. Relationship between the stock time and H_2O_2 concentration.

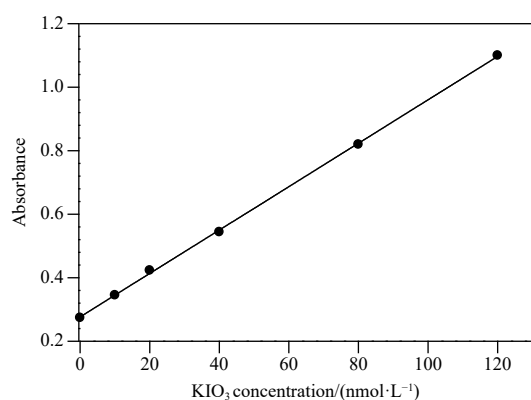


Fig. 7. Relationship between iodate concentration and absorbance measured by LWCC in artificial seawater.

sorptivity of the above standard curve was $(22\,958 \pm 285) \text{ L}/(\text{mol}\cdot\text{cm})$, which is comparable with that of the conventional method.

Spectrometric methods are influenced by the salinity effect, i.e., the molar absorptivity decreases with the increase in salinity. Therefore, the salinity of the standard curves must be adjusted similarly to that of the samples. However, establishing standard curves with numerous, small salinity intervals is difficult. Hence, examining how the salinity difference between the standard curve and the samples results in acceptable errors is necessary. The results show that the difference between salinity 35 and 0 was approximately 6% (Fig. 8). Therefore, the salinity difference between the standard curves and the samples must be within 5 to offset the salinity effect and minimize the resulting error to within 1%, which is lower than the method's precision.

Table 1 lists the precision of iodate measurements in different intermediates (artificial seawater or natural estuarine water). Within-run precision of repeatability was determined by analyzing five samples. The results show that in artificial seawater, 0.01 $\mu\text{mol}/\text{L}$, 0.02 $\mu\text{mol}/\text{L}$, 0.06 $\mu\text{mol}/\text{L}$, and 0.08 $\mu\text{mol}/\text{L}$ iodate were detected, with standard deviations (SD) of 0.002 $\mu\text{mol}/\text{L}$, relative standard deviation (RSD) of 7.3%, and recovery ratio of 97.6%–

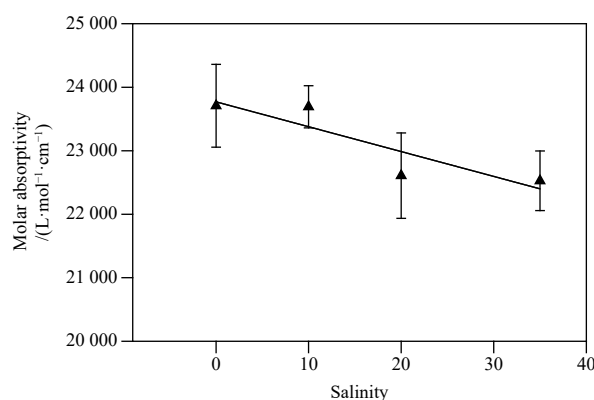


Fig. 8. Relationship between the molar absorptivity of the standard curves and the salinity in a LWCC system, $\varepsilon = -39.1\text{salinity} + 23\,770$.

103.7%. In natural waters, when iodate was 0.011 $\mu\text{mol}/\text{L}$, the RSD was 15%, which is higher than in the artificial seawater. When the iodate concentration was higher than 0.03 $\mu\text{mol}/\text{L}$, the two intermediates showed no difference, i.e., the method can be applied to natural waters.

The SD, RSD, and recovery of several levels of iodate solution are listed in Table 1; detection limit is $\sim 2 \text{ nmol}/\text{L}$, and quantification limit is 9 nmol/L .

3.4 Sample analysis

The developed method was applied to several estuarine and coastal water samples (Table 2). The salinity difference between a sample and the standard curve was 5 on average. All samples were measured using conventional spectrophotometry and LWCC for comparison. The coastal waters and part of estuarine water samples measured by LWCC were diluted to the measuring range when needed. The results show that the concentrations measured by LWCC and conventional spectrophotometer were within 7%. Given the established efficacy of the conventional spectrophotometric method, this finding proves that the spectrometric

Table 1. Precision and recovery ratio of spectrophotometric method to measure iodate with LWCC

Sample	Iodate added $/(\text{nmol}\cdot\text{L}^{-1})$	Iodate measured concentration $/(\text{nmol}\cdot\text{L}^{-1})$	Average $/(\text{nmol}\cdot\text{L}^{-1})$	SD $/(\text{nmol}\cdot\text{L}^{-1})$	RSD/%	Recovery/%
Artificial seawater	0	2.1, 0.6, 1.0	1.2	1.1	–	–
	10	9.8, 10.9, 10.4	10.4	0.6	5.3	104.0
	20	20.4, 18.6, 19.6	19.5	0.9	4.6	97.7
	40	38.8, 42.6, 36.9	39.4	2.9	7.4	98.5
	80	80.8, 82.8, 82.1	82.0	1.0	2.1	102.5
Danshui Estuary 1	–	9, 12	11	2.1	15.0	–
Danshui Estuary 2	–	31, 29, 30	30	1.0	3.0	–

Note: SD represents standard deviation; RSD, relative standard deviation; the intermediate is artificial seawater; –, no data.

Table 2. Comparison of the results of spectrometric methods to measure iodate with LWCC or conventional spectrophotometer

Site	Latitude	Longitude	Salinity	Measured by LWCC $/(\text{nmol}\cdot\text{L}^{-1})$	Measured by conventional method $/(\mu\text{mol}\cdot\text{L}^{-1})$
Danshui Estuary	25.169 5°N	121.439 0°E	14.84	62±2	0.06±0.01
			15.54	67±2	0.07±0.01
Changjiang Estuary	31.241 3°N	122.020 5°E	1.73	0±2	0±0.01
			7.57	0±2	0±0.01
			11.40	18±2	0±0.01
			13.64	62±2	0.06±0.01
Jiulong Estuary	24.401 3°N	117.961 3°E	6.30	11±2	0±0.01

method based on LWCC is dependable. In addition, its measurement values for trace iodate in water samples from Jiulong Estuary (11 nmol/L) and Changjiang Estuary (18 nmol/L) were authentic.

4 Conclusions

A new method based on LWCC is developed to measure nanomolar iodate concentration in environmental samples. This novel technique promoted the sensitivity of determination with a low detection limit and presented good spiked recoveries are good. The promoted and conventional methods were applied in water samples from several estuaries and coastal ocean.

Acknowledgements

The author is grateful for the help of the Research Center for Environmental Change. Comments supplied by two anonymous reviewers have been proven invaluable in the completion of this manuscript.

References

- Bricaud A, Morel A, Prieur L. 1981. Absorption by dissolved organic matter of the sea (yellow substance) in the UV and visible domains. *Limnology and Oceanography*, 26(1): 43–53, doi: [10.4319/lo.1981.26.1.0043](https://doi.org/10.4319/lo.1981.26.1.0043)
- Brüchert W, Helfrich A, Zinn N, et al. 2007. Gel electrophoresis coupled to inductively coupled plasma-mass spectrometry using species-specific isotope dilution for iodide and iodate determination in aerosols. *Analytical Chemistry*, 79(4): 1714–1719, doi: [10.1021/ac061767y](https://doi.org/10.1021/ac061767y)
- Carpenter J H. 1965. The accuracy of the Winkler method for dissolved oxygen analysis. *Limnology and Oceanography*, 10(1): 135–140, doi: [10.4319/lo.1965.10.1.0135](https://doi.org/10.4319/lo.1965.10.1.0135)
- Chapman P, Liss P S. 1977. The effect of nitrite on the spectrophotometric determination of iodate in seawater. *Marine Chemistry*, 5(3): 243–249, doi: [10.1016/0304-4203\(77\)90019-6](https://doi.org/10.1016/0304-4203(77)90019-6)
- Cutter G A, Moffett J G, Nielsdottir M C, et al. 2018. Multiple oxidation state trace elements in suboxic waters off Peru: *in situ* redox processes and advective/diffusive horizontal transport. *Marine Chemistry*, 201: 77–89, doi: [10.1016/j.marchem.2018.01.003](https://doi.org/10.1016/j.marchem.2018.01.003)
- Dubravčić M. 1955. Determination of iodine in natural waters. *Analyst*, 80(949): 295–300, doi: [10.1039/AN9558000295](https://doi.org/10.1039/AN9558000295)
- Fitzmaurice D J, Frei H. 1991. Transient near-infrared spectroscopy of visible light sensitized oxidation of iodide at colloidal titania. *Langmuir*, 7(6): 1129–1137, doi: [10.1021/la00054a019](https://doi.org/10.1021/la00054a019)
- Guo Jianbao, Peng Zhen. 1989. Geochemical behaviour of iodine in Jiulong River Estuary. *Acta Oceanologica Sinica*, 8(1): 91–99
- Guo Weidong, Stedmon C A, Han Yuchao, et al. 2007. The conservative and non-conservative behavior of chromophoric dissolved organic matter in Chinese estuarine waters. *Marine Chemistry*, 107(3): 357–366, doi: [10.1016/j.marchem.2007.03.006](https://doi.org/10.1016/j.marchem.2007.03.006)
- Herring J R, Liss P S. 1974. A new method for the determination of iodine species in seawater. *Deep Sea Research and Oceanographic Abstracts*, 21(9): 777–783, doi: [10.1016/0011-7471\(74\)90085-0](https://doi.org/10.1016/0011-7471(74)90085-0)
- Kieber R J, Helz G R. 1992. Indirect photoreduction of aqueous chromium (VI). *Environmental Science & Technology*, 26(2): 307–312
- Lyman J, Fleming R H. 1940. Composition of seawater. *Journal of Marine Research*, 3(2): 131–146
- Moriyasu R, Evans N, Bolster K M, et al. 2020. The distribution and redox speciation of iodine in the eastern Tropical North Pacific Ocean. *Global Biogeochemical Cycles*, 34(2): e2019GB006302
- Pai Sucheng, Gong G C, Liu K K. 1993. Determination of dissolved oxygen in seawater by direct spectrophotometry of total iodine. *Marine Chemistry*, 41(4): 343–351, doi: [10.1016/0304-4203\(93\)90266-Q](https://doi.org/10.1016/0304-4203(93)90266-Q)
- Schwehr K A, Santschi P H. 2003. Sensitive determination of iodine species, including organo-iodine, for freshwater and seawater samples using high performance liquid chromatography and spectrophotometric detection. *Analytica Chimica Acta*, 482(1): 59–71, doi: [10.1016/S0003-2670\(03\)00197-1](https://doi.org/10.1016/S0003-2670(03)00197-1)
- Smith J D, Butler E C V. 1979. Speciation of dissolved iodine in estuarine waters. *Nature*, 277(5696): 468–469, doi: [10.1038/277468a0](https://doi.org/10.1038/277468a0)
- Tian R C, Marty J C, Nicolas E, et al. 1996. Iodine speciation: a potential indicator to evaluate new production versus regenerated production. *Deep-Sea Research Part I: Oceanographic Research Papers*, 43(5): 723–738, doi: [10.1016/0967-0637\(96\)00023-4](https://doi.org/10.1016/0967-0637(96)00023-4)
- Truesdale V W. 1994. Distribution of dissolved iodine in the Irish Sea, a temperate shelf sea. *Estuarine, Coastal and Shelf Science*, 38(5): 435–446
- Truesdale V W, Bailey G W. 2002. Iodine distribution in the Southern Benguela system during an upwelling episode. *Continental Shelf Research*, 22(1): 39–49, doi: [10.1016/S0278-4343\(01\)00075-9](https://doi.org/10.1016/S0278-4343(01)00075-9)
- Tsunogai S. 1971. Iodine in the deep water of the ocean. *Deep Sea Research and Oceanographic Abstracts*, 18(9): 913–919, doi: [10.1016/0011-7471\(71\)90065-9](https://doi.org/10.1016/0011-7471(71)90065-9)
- Tsunogai S, Henmi T. 1971. Iodine in the surface water of the ocean. *Journal of the Oceanographical Society of Japan*, 27(2): 67–72, doi: [10.1007/BF02109332](https://doi.org/10.1007/BF02109332)
- Ullman W J, Luther G W, Aller R C, et al. 1988. Dissolved iodine behavior in estuaries along the east coast of the United States. *Marine Chemistry*, 25(2): 95–106, doi: [10.1016/0304-4203\(88\)90058-8](https://doi.org/10.1016/0304-4203(88)90058-8)
- Wong G T F. 1976. *Dissolved Inorganic and Particulate Iodine in the Oceans*. Cambridge, MA: Massachusetts Institute of Technology
- Wong G T F. 1991. The marine geochemistry of Iodine. *Critical Reviews in Aquatic Sciences*, 4(1): 45–73
- Wong G T F. 1995. Dissolved iodine across the Gulf Stream Front and in the South Atlantic Bight. *Deep-Sea Research Part I: Oceanographic Research Papers*, 42(11–12): 2005–2023
- Wong G T F, Brewer P G. 1974. The determination and distribution of iodate in South Atlantic waters. *Journal of Marine Research*, 32(1): 25–36
- Wong G T F, Brewer P G, Spencer D W. 1976. The distribution of particulate iodine in the Atlantic Ocean. *Earth and Planetary Science Letters*, 32(2): 441–450
- Wong G T F, Cheng Xianhao. 1998. Dissolved organic iodine in marine waters: Determination, occurrence and analytical implications. *Marine Chemistry*, 59(3–4): 271–281
- Wong G T F, Cheng Xianhao. 2001. Dissolved organic iodine in marine waters: role in the estuarine geochemistry of iodine. *Journal of Environmental Monitoring*, 3(2): 257–263, doi: [10.1039/b007229j](https://doi.org/10.1039/b007229j)
- Wong G T F, Cheng Xianhao. 2008. Dissolved inorganic and organic iodine in the Chesapeake Bay and adjacent Atlantic waters: speciation changes through an estuarine system. *Marine Chemistry*, 111(3–4): 221–232
- Wong G T F, Zhang Lingsu. 2003. Seasonal variations in the speciation of dissolved iodine in the Chesapeake Bay. *Estuarine, Coastal and Shelf Science*, 56(5–6): 1093–1106
- Wu Man, Wong G T F, Wu Yaochu, et al. 2015. Hydrogen peroxide in tropical shelf waters: the northern South China Sea Shelf. *Deep-Sea Research Part II: Topical Studies in Oceanography*, 117: 143–154, doi: [10.1016/j.dsr2.2015.02.027](https://doi.org/10.1016/j.dsr2.2015.02.027)
- Xie Weiqi, Yu Kongxian, Gong Yixian. 2019. Determination of iodate in iodized edible salt based on a headspace gas chromatographic technique. *Journal of Chromatography A*, 1584: 187–191, doi: [10.1016/j.chroma.2018.12.009](https://doi.org/10.1016/j.chroma.2018.12.009)
- Zhang Ya'nan, Yu Hong, Ma Yajie, et al. 2018. Imidazolium ionic liquids as mobile phase additives in reversed phase liquid chromatography for the determination of iodide and iodate. *Analytical and Bioanalytical Chemistry*, 410(28): 7347–7355, doi: [10.1007/s00216-018-1347-5](https://doi.org/10.1007/s00216-018-1347-5)